Journal of Modern Transportation
Volume 20, Number 2, June 2012, Page 65-69
Journal homepage: jmt.swjtu.edu.cn
DOI: 10.1007/BF03325779

Defect control at nanoscale and flux pinning enhancement in MgB_2 superconductor

C.H. CHENG*, C. SORRELL

School of Materials Science and Engineering, University of New South Wale, Sydney 2052, NSW, Australia

Abstract: Defect control at nanoscale of MgB_2 by doping various nanoparticles including Ti, C, nano-diamond, and HoB_4, and their roles played to enhance flux pinning force in MgB_2 are compared and analyzed. These nanodopants have different chemical and physical properties, thus bring about different pinning efficiency, especially nanodopants with strong magnetic moment are particularly interesting as pinning centers in MgB_2 since magnetic impurities usually have a stronger interaction with magnetic flux line than nonmagnetic impurities and may exert a stronger force to trap the flux lines when they are properly introduced into the superconducting matrix.

Key words: MgB_2; flux pinning; nano-pinning centers; microstructure control

1. Introduction

Large-scale superconducting devices for power applications depend on the conductors with high critical current densities at temperatures where the costs for coolant are affordable. The discovery of superconductivity at 39 K in MgB_2 [1] offers the possibility of wide engineering applications in a temperature range of 20–30 K, where the conventional superconductors cannot play any roles because of low T_c. However, the commercialization of MgB_2-based superconducting technology depends critically on continuous improvement of the performance of MgB_2 material, especially the properties in high magnetic fields, including H_{c2} and J_c.

Among many methods, alloying with carbon seems to be the most effective to improve the H_{c2} by shorting the mean free length of electron [2]. Besides the efforts of increasing H_{c2} by carbon doping, many efforts have been focused on the control of nanostructure of MgB_2 in order to introduce nano-pinning-centers in the system and then increase the J_c. There are a variety of types of nanoparticles used to doping the MgB_2 matrix and modify its nanostructure in order to control the pinning structure of the MgB_2 superconductors. Typical nanoscale doping materials used for this purpose include Ti, Zr, nano-diamond, HoB_4, etc., and their effects on flux pinning behavior of MgB_2 are quite striking [3-7]. However, the chemical and/or physical properties of these nanodopants are very different from each other, the underpinning mechanisms are not well understood up to date, thus it is necessary to clarify them in order to optimize the nano-pinning structure for a better performance.

In this paper, magnetic and nonmagnetic nanopartical doping effect has been analyzed against their flux pinning behavior for MgB_2 superconductor. We identify that nanodopants with strong magnetic moment are particularly interesting as pinning centers in MgB_2 since magnetic impurities usually have a stronger interaction with magnetic flux line than nonmagnetic impurities and may exert a stronger force to trap the flux lines when they are properly introduced into the superconducting matrix. This suggests that pinning sites with strong magnetic moment may play an important role to further improve the pinning behavior of MgB_2 in practical applications.

2. Experimental

Typical procedures for the preparation of the samples are: samples with a nominal composition are prepared with solid state reaction method with starting powder materials of amorphous B (99.99%), Mg (99.9%), and the nano-particle dopants. The particle sizes of magnesium and boron are about 1 Micron and 200 nm, respectively. The size of the nano dopants is about 10–50 nm. After well ground in a glove box for 1 h, the mixed powders were pressed into pellets of a diameter of 10 mm, sealed in iron tubes with excess Mg, sintered at 850 °C for 2 h in flowing Ar, and finally quenched to room temperature.

Received May 10, 2012; revision accepted Jun. 6, 2012
*Corresponding author. E-mail: chengcecily@gmail.com (C.H. CHENG)

doi: 10.3969/j.issn.2095-087X.2012.02.001

Crystalline structure was studied by powder X-ray diffraction (XRD) using an X'Pert MRD diffractometer with Cu *K*-alpha radiation. Microstructure was analyzed with a scanning electron microscope (SEM) and a Philips field emission transmission electron microscope with energy-dispersive X-ray spectroscopy (EDX) analysis. Magnetization was measured using a 9 T physical property measurement system (Quantum design). The typical sample size is $0.8\times0.8\times1.0$ mm^3. A magnetic J_c was derived from the width of the magnetization loop ΔM based on the extended Bean model: $J_c=20\Delta M/[a(1-a/3b)]$. H_{irr} was determined from emerging point of $M(T)$ curve measured in zero-field-cooling (ZFC) and field-cooling (FC) processes at various fields up to 7 T.

3. Results and discussion

3.1. Nano-diamond doping effect

The MgB_2-diamond nanocomposites with compositions of $MgB_{2-x}C_x$ (x=0%, 5%, 8%, and 10%) were prepared. The size of nanodiamond powder is ~10–20 nm. These samples were sintered at a relatively high temperature of 800 °C for a relatively long time of 2 h in order to emphasize the carbon substitution effect on B. Another sample with an added 1.5 wt% of nanodiamond in MgB_2 was also prepared but at a relatively low temperature of 730 °C for a relatively short time of 30 min in order to reduce the substitution effect of carbon in boron in MgB_2 and emphasize the additional effect of the nanodiamond in MgB_2.

As shown in Fig. 1(a), the diamond substitutional sample mainly consists of relatively large MgB_2 grains (~1 μm in size) with a high density of dislocations. In some areas, discrete nano-sized particles can be observed. These dislocations mainly occur near the nanodiamond particles. This clearly shows that the unreacted carbon can introduce high density of dislocation loops in the MgB_2 matrix. This phenomenon was first noted in 2003 [8-10], but its effect was not fully recognized.

As shown in Fig. 1(b), these nano-diamond doped samples exhibit significant improvements of J_c, especially in high magnetic field and low temperature rejoin. This can be attributed to the substitution effect of C which enhances H_{c2}, thus consequently J_c. The C substation effect is usually due to the impurity scattering effect on electrons. What we would like to point out here, the high density of dislocations induced by nanodiamond may also introduce structure-imperfection scattering effect on electrons which also enhances the H_{c2} of the system. Such a dislocation enhanced H_{c2} should be paid attention in MgB_2 system as an alternative of improving the performance of the superconductor.

Different from the diamond substitutional sample which mainly consists of relatively large MgB_2 grains (~1 μm) with a high density of dislocations, the diamond-added sample mainly consists of two kinds of nanoparticles: MgB_2 grains with a size of 50–100 nm and diamond particles with a size of 10–20 nm (the results are not shown here). In fact, this diamond-added MgB_2 forms a typical nano-composite material.

The nano-diamond particles are inserted into the MgB_2 grains. As the *ab*-plane coherence length of MgB_2 is about 6–7 nm [11], these 10 to 20-nm-sized diamond inclusions, with a high density, are ideal flux pinning centers and are responsible for the high performance in our samples. The effect of diamond doping on the enhancement of flux pinning in MgB_2 can be counterbalanced by its suppression on superconductivity, as clearly shown in the situation of T=30 K. This counterbalancing effect

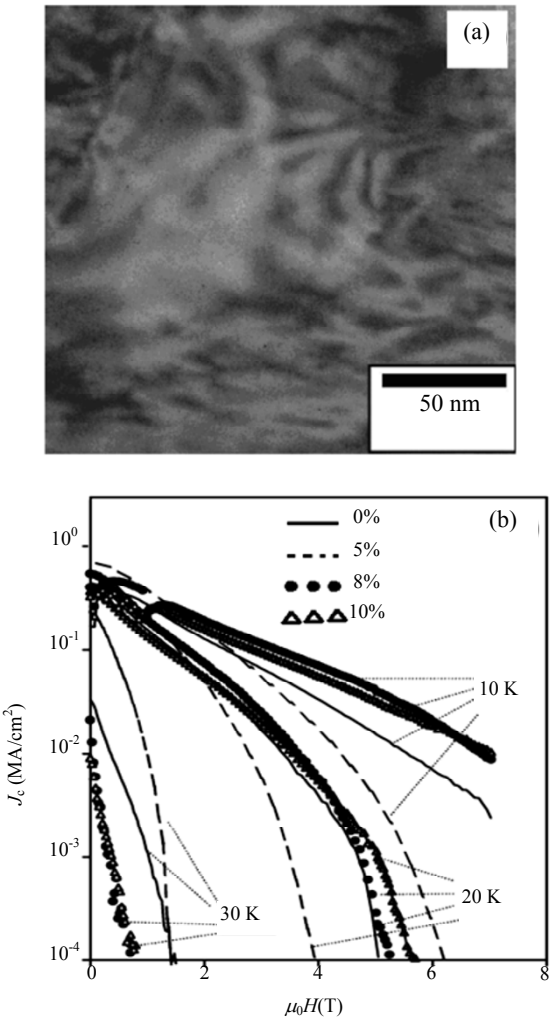

Fig. 1 (a) FEGTEM micrographs for: diamond-substituted MgB_2 with x=5%. (b) Magnetic field dependence of J_c at 10, 20 and 30 K for nano-diamond substituted MgB_2 with x=0% (dashed lines), 5% (solid lines), 8% (solid circles) and 10% (opened triangles).

may also exist at other temperatures, even when the effect of the J_c enhancement is dominant. The further increase of J_c depends critically on reducing the T_c-suppression effect in the MgB_2-diamond composite. This idea is confirmed by the results obtained in the diamond-added sample, 1.5 wt% C, which has a higher T_c than other diamond-doped samples and contains more nanodiamond inclusions as revealed by the transmission electron microscopy analysis. As revealed experimentally, the diamond-added sample shows a much better J_c-H behavior than the carbon-substituted sample. Its J_c reaches 1×10^4 A/cm^2 at 20 K and 4 T, and its H_{irr} reaches 6.4 T at 20 K. In fact, at all temperatures below 35 K, the J_c-H behavior (results at 20 K are shown here only) and the H_{irr}-T relation of the diamond-added sample are much better than those of other samples in this study.

3.2. Carbon and Ti concurrent doping effect

Although carbon doping can significantly increase the upper critical field of MgB_2, and thus improve the J_c-H behavior at high field, however, the critical current density J_c of MgB_2 bulks sintered at ambient pressure is still inferior to the conventional A15 compound superconductors and Nb-Ti due to a poor connection between grains and the lack of flux pinning centers in the materials. It is expected that the pinning behavior in carbon-doped MgB_2 may be further improved if its microstructure can be improved. Ti may be a good candidate for this purpose since doping Ti in MgB_2 could highly improve the superconducting properties of MgB_2 in low field by controlling the microstructure of MgB_2 (see Fig. 2) [4-5]. Therefore, it is very possible to improve both H_{c2} and J_c of MgB_2 simultaneously by concurrently doping carbon and Ti, thus further improving its performance, especially in the higher magnetic field regime.

By taking the advantages of concurrent doping of Ti and C, the microstructure of Ti-C-doped MgB_2 is further improved. The inset of Fig. 3 shows the typical magnetization hysteresis loops measured at 20 K for the undoped, Ti-doped, and C-Ti- doped MgB_2 samples and the $J_c(H)$ curves for the typical samples at T=20 K. Magnetization hysteresis loops at 10 and 5 K are similar to those at 20 K. In this study, the focus is the improvement of superconducting performance at 20 K because, at this temperature, the conventional superconductors, such as Nb_3Sn and Nb-Ti alloy, can no longer be used due to a lower T_c. For the undoped MgB_2, magnetization hysteresis loop is relatively narrow and small, suggesting a relatively low J_c and a low irreversibility field H_{irr}. After it was doped with Ti, the loop width, ΔM is significantly enlarged at low fields. However, the loop width decreases rapidly with increasing the applied magnetic field, suggesting a degradation of the flux pinning in the magnetic field. By further doping C in Ti-doped MgB_2, the rapid decrease of ΔM is suppressed.

As shown in the main panel of Fig. 3, the in-field critical current densities were enhanced by Ti doping, particularly in lower fields. At 20 K, the maximum zero field value $J_c(0)$ was achieved in $Mg_{0.95}Ti_{0.05}B_2$ sample, and a J_c value in self-field at 20 K was improved from 2.1×10^5 A/cm^2 of undoped sample to 3.1×10^5 A/cm^2. This result is consistent with the result of Ti-doped MgB_2 bulk superconductor, where $J_c(0)$ was improved by refining MgB_2 grains and forming a strongly coupled nanoparticle structure [5].

The most striking feature shown in Fig. 3 is that the C-Ti-doped sample exhibited the combined benefits of C and Ti. The J_c values of this sample is lower than that of Ti-doped sample in magnetic field from 0 to 2 T, but in higher magnetic fields ($>$2 T), its J_c is significantly improved and much higher than the J_c of Ti-doped sam-

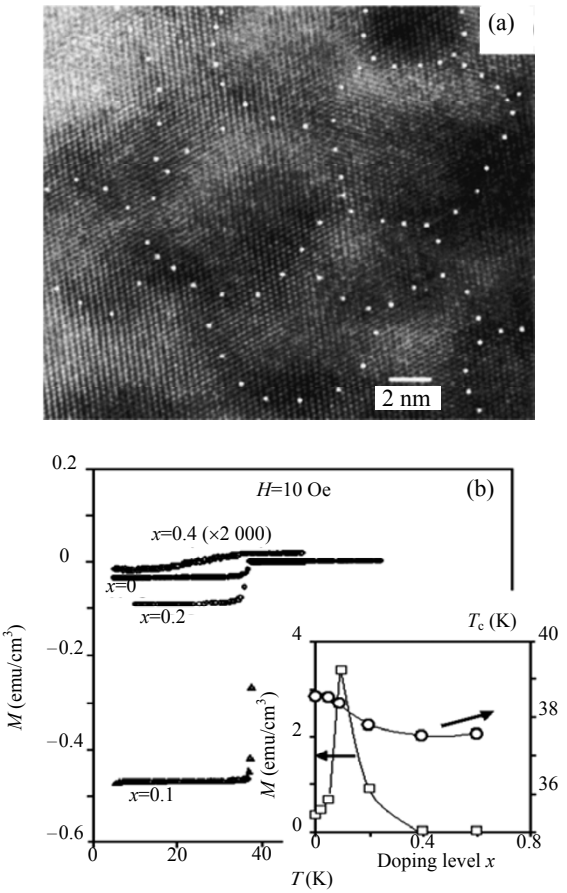

Fig. 2 HRTEM photograph for Ti-doped MgB_2 (x=10%). A dotted network is drawn for convenience to enable one to see the nanoparticle structure. (b) Volume magnetization vs temperature curves for Ti-doped MgB_2 with doping levels of x=0, 0.1, 0.2, and 0.4, measured at 10 Oe in the ZFC process. The data for the sample with x=0.4 are multiplied by a factor of 2 000. Inset: variation of critical temperature T_c and the diamagnetic signal represented by the volume magnetization at 5 K and 10 Oe with doping level x for Ti-doped MgB_2 samples.

ple. Accordingly, the irreversibility field is also significantly improved. What is more, this sample showed a better in-field J_c than carbon doped samples, including nanocarbon-doped MgB_2 [12] and CNT-doped MgB_2 [13] in the high magnetic field region. At temperature of 20 K, the J_c reaches 1×10^4 A/cm^2 in 4 T, and 4×10^3 A/cm^2 in 5 T; and the irreversibility field determined from the closure of hysteresis loops with a criterion of 10^2 A/cm^2 exceeds 6 T. This is one of the best values for MgB_2 at 20 K.

3.3. Nano Ho_2O_3 doping effect

Magnetic impurities, as an easy way for magnetic flux penetration, will exert a stronger force to trap the flux lines if they can be properly introduced into the superconducting matrix. Therefore, pinning sites with strong magnetic moment is always of interest to explore the new route to enhance the pinning behavior of MgB_2.

As shown in Fig. 4, SEM micrograph shows that the samples are tightly packed MgB_2 nanoparticle structure with an average particle size of 50–100 nm.

As mentioned previously this type of nanostructure in MgB_2 provides a good grain connection as well as the grain boundary flux pinning, sustaining a high J_c in low and medium high field regions (＜4 T) for MgB_2. Further, TEM micrograph reveals that highly disperse nanoparticles with a size of 5–10 nm are inserted in the MgB_2 matrix. EDX analysis reveals that these nanopar ticles contain mainly Ho and B. Combining with the XRD analyses it can be deduced that these nanoparticles are HoB_4 [14-15]. This clearly confirms that doping Ho_2O_3 nanoparticles results in the formation of HoB_4 nanoparticles which are weak magnetic in physical properties.

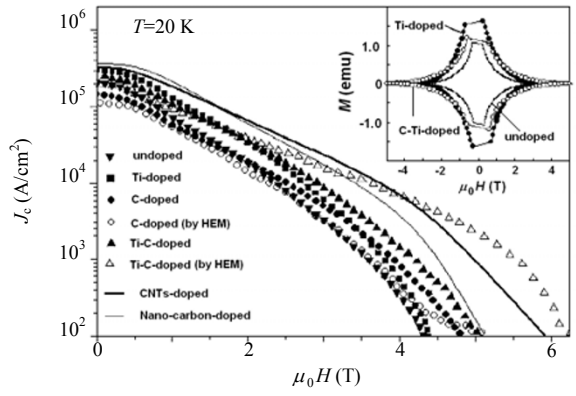

Fig. 3 $J_c(H)$ behavior at T=20 K for the undoped, Ti-doped, C-doped, and C-Ti-doped samples. For the sake of comparison, the J_c results of nanocarbon-doped MgB_2 [12] and CNT-doped MgB_2 are plotted in the figure. Inset: Magnetization hysteresis loops at T=20 K for undoped, Ti-doped, and C-Ti-doped samples.

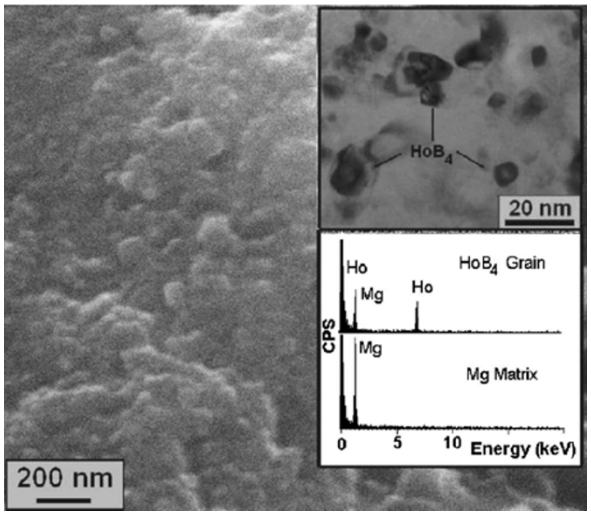

Fig. 4 TEM micrograph which shows the HoB_4 nano-dots inserting in the MgB_2 matrix, and EDX patterns for the nanoparticle shown in the TEM micrograph.

Fig. 5 shows the $J_c(H)$ curves for $Mg_{1-x}(Ho_2O_3)_xB_2$ samples at 5 K, 10 K and 20 K. In the low-field region, the heavily-doped samples exhibit a J_c slightly lower than that of the undoped MgB_2. However, at all temperatures studied in this work, the in-field critical current densities have been enhanced by Ho_2O_3 doping in high field region. The enhancement of J_c is getting more drastic with increasing doping level at $x\leqslant3\%$, but it begins to debase at x=10%, suggesting an optimal doping level for the J_c enhancement is between 3% and 10%. In a field of 5 T, the 3%-doped MgB_2 sample reaches a J_c of 1.0×10^3 A/cm^2 at 20 K, 2.0×10^4 A/cm^2 at 10 K and 1.2×10^5 A/cm^2 at 5 K.

Different from the doping effect of non-magnetic or weak magnetic impurities on MgB_2, such as Ti, Zr, Dy_2O_3, and Y_2O_3 [3-7], which mainly improves the J_c in lower field region, Ho_2O_3 doping does not improve the low-field J_c significantly, but results in a significant improvement on J_c in higher field region. At T=5 K, the J_c values of Ti- and Dy_2O_3-doped MgB_2 are much higher than that of Ho_2O_3-doped sample when applied field is lower than 2 T; however, these J_c values decrease rapidly with further increasing the applied field, reaching a J_c value much lower than that of Ho_2O_3-doped sample in a field higher than 4 T. For example, at 5 K, both 10%Ti- and 3%Ho_2O_3-doped MgB_2 have a J_c around 2.0×10^5 A/cm^2 in a field of 4 T, but the J_c for Ti-doped one drops to a value around 9.0×10^3 A/cm^2 at 6.5 T whereas Ho_2O_3-doped sample keeps a value higher than 7.0×10^4 A/cm^2, which is about 8 time higher. Further increasing the applied field to 9 T, the Ho_2O_3-doped sample can still sustain a J_c as high as 3.0×10^4 A/cm^2. The improvement of J_c-H behavior of MgB_2 by Ho_2O_3 doping is also comparable with that achieved by nano-

carbon-doped MgB_2 in magnetic fields lower than 9 T [16] (see Fig. 5).

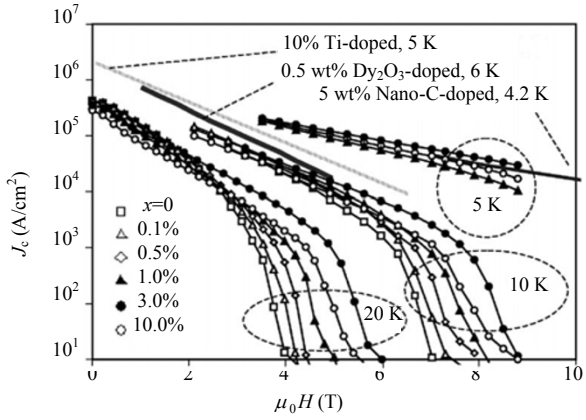

Fig. 5 Field dependence of magnetic J_c at 5, 10, and 20 K for $Mg_{1-x}(Ho_2O_3)_xB_2$ samples with various doping levels [14-15].

4. Conclusions

From the comparison of recent research results on the nanostructural control of MgB_2 by doping various nanoparticles including Ti, nano-diamond, and Ho_2O_3, and their effects on flux pinning behavior of MgB_2 some interesting conclusions can be drawn. (1) By nanodiamond doping, the diamond-MgB_2 nano-composite superconductor forms, which consists of tightly-packed MgB_2 nano-grains (~50–100 nm) with highly dispersed and uniformly distributed diamond nanoparticles (~10–20 nm) inside the grains. (2) Carbon and Ti concurrently doping are largely cooperative in improving the performance of MgB_2 in the high magnetic fields (>3 T) and at high temperature (~20 K). (3) In Ho_2O_3 doped samples, the magnetic HoB_4 nanoparticles were attributed to be the source for the enhanced flux pinning effects. (4) Magnetic pinning centers show the most effective pinning behavior amongst those mentioned above and should be paid close attention in the practical applications.

Acknowledgment

This work was supported Australian Research Council (Nos. DP0559872 and DP0881739).

References

[1] J. Nagamatsu, N. Nakagawa, T. Muranaka, et al., Superconductivity at 39 K in magnesium diboride, *Nature*, 2001, **410**: 63-64.

[2] A. Gurevich, Enhancement of the upper critical field by nonmagnetic impurities in dirty two-gap superconductors, *Physical Review B*, 2003, **67**(18): 1-13.

[3] J. Wang, Y. Bugoslavsky, A. Berenov, et al., High critical current density and improved irreversibility field in bulk MgB_2 made by a scaleable, nanoparticle addition route, *Applied Physics Letters*, 2002, **81**(11): 2026-2028.

[4] Y. Zhao, D. X. Huang, Y. Feng, et al., Nanoparticle structure of MgB_2 with ultrathin TiB_2 grain boundaries, *Applied Physics Letters*, 2002, **80**(9): 1640-1642.

[5] Y. Zhao, Y. Feng, C. H. Cheng, et al., High critical current density of MgB_2 bulk superconductor doped with Ti and sintered at ambient pressure, *Applied Physics Letters*, 2001, **79**(8)**:** 1154-1156.

[6] S.K. Chen, M. Wei, J.L. MacManus-Driscoll, Strong pinning enhancement in MgB_2 using very small Dy_2O_3 additions, *Applied Physics Letters*, 2006, **88**(19): 192512-19512-3.

[7] Y. Feng, Y. Zhao, Y.P. Sun, et al., Improvement of critical current density in MgB_2 superconductors by Zr doping at ambient pressure, *Applied Physics Letters*, 2001, **79**(24): 3983-3985.

[8] C.H. Cheng, H. Zhang, Y. Zhao, et al., Doping effect of nano-diamond on superconductivity and flux pinning in MgB_2, *Superconductor Science and Technology*, 2003, **16**(10), 1182-1186.

[9] Y. Zhao, C.H. Cheng, X.F. Rui, et al., Improved irreversibility behavior and critical current density in MgB2-diamond nanocomposites, *Applied Physics Letters*, 2003, **83**(14): 2916-2918.

[10] C.H. Cheng, Y. Yang, P. Munroe, et al., Comparison between nano-diamond and carbon nanotube doping effects on critical current density and flux pinning in MgB_2, *Superconductor Science and Technology*, 2007, **20**(3): 296-301.

[11] M. Xu, H. Kitazawa, Y. Takano, et al., Anisotropy of superconductivity from MgB_2 single crystals, *Applied Physics Letters*, 2001, **79**(17): 2779-2781.

[12] S. Soltanian, J. Horvat, X.L. Wang, et al., Effect of nano-carbon particle doping on the flux pinning properties of MgB_2 superconductor, *Physica C: Superconductivity*, 2003, **390**(3): 185.

[13] S.X. Dou, W.K. Yeoh, J. Horvat, et al., Effect of carbon nanotube doping on critical current density of MgB2 superconductor, *Applied Physics Letters*, 2003, **83**(24): 4996-4998.

[14] C. Cheng, Y. Zhao, Significant improvement of flux pinning and irreversibility field of nano-Ho_2O_3 doped MgB_2, *Physica C: Superconductivity*, 2007, **463-465**: 220-224.

[15] C. Cheng, Y. Zhao, Enhancement of critical current density of MgB_2 by doping Ho_2O_3, *Applied Physics Letters*, 2006, **89**(25): 252501-252501-3.

[16] Y.W. Ma, X.P. Zhang, G. Nishijima, et al., Significantly enhanced critical current densities in MgB_2 tapes made by a scaleable nanocarbon addition route, *Applied Physics Letters*, 2006, **88(7):** , 072502-072502-2.

(Editor: Yao ZHOU)